IEEE Access
Multidisciplinary ⋮ Rapid Review ⋮ Open Access Journal

Received 30 January 2023, accepted 10 March 2023, date of publication 22 March 2023, date of current version 29 March 2023.

Digital Object Identifier 10.1109/ACCESS.2023.3260252

RESEARCH ARTICLE

Tikhonov Regularization and Perturbation-Level Tuning for the CNM in Pharmacokinetics

LUONG THI THEU[1], TRAN QUANG-HUY[2], TRAN DUC-TAN[3], (Member, IEEE), BHISHAM SHARMA[4], SUBRATA CHOWDHURY[5], (Member, IEEE), KARTHIK CHANDRAN[6], (Senior Member, IEEE), AND SARAVANAKUMAR GURUSAMY[7], (Senior Member, IEEE)

[1]Institute of Applied Technology, Thu Dau Mot University, Binh Duong, Vietnam
[2]Faculty of Physics, Hanoi Pedagogical University 2, Hanoi, Vietnam
[3]Faculty of Electrical and Electronic Engineering, Phenikaa University, Hanoi 12116, Vietnam
[4]Chitkara University Institute of Engineering and Technology, Chitkara University, Punjab 140401, India
[5]Department of Computer Science and Engineering, Sreenivasa Institute of Technology and Management Studies, Chittoor, Andhra Pradesh 517127, India
[6]Robotics and Automation, Jyothi Engineering College, Cheruthuruthi 679531, India
[7]Department of Electrical and Electronics Technology, FDRE Technical and Vocational Training Institute, Addis Ababa 620310, Ethiopia

Corresponding author: Saravanakumar Gurusamy (saravanakumar.gurusamy@etu.edu.et)

ABSTRACT In pharmacokinetics, the clinical information collected from the patient is often much less than the complexity of the patient's internal operations, hence the undetermined inverse problem has emerged as a challenge to solve it and find multiple possible point sets for considering the many possible implications of drug kinetics in the patient's body. This paper suggests two enhanced schemes for the early cluster Newton method (CNM) to concomitantly explore a great solutions number for the inverse parameter determination in pharmacokinetics. The first scheme is the application of Tikhonov regularization to deal with the overdetermined system for hyperplane fitting in the CNM, and the second is an effective iterative strategy by tuning perturbation-level for the CNM. As a result of Tikhonov's filtering operation, lower order singular values than the regularization parameter, that are to blame for the instability of the matrix equation, are efficiently eliminated. With perturbation-level tuning, following every iteration, as the point cluster (PoC) gets near the solution manifold (SoM), it is essential to lessen the level of perturbation in the patient's clinical measurement data and this is suited for a numerical stabilization. Numerical simulation scenarios of two schemes have revealed that these suggested schemes can lower the iterations number and computed time, and PoC move more steadily towards the solutions manifold.

INDEX TERMS Tikhonov regularization, physiologically based pharmacokinetics, pharmacokinetics, cluster Newton method, inverse problem.

I. INTRODUCTION

In pharmacokinetics, we frequently encounter the problem of underdetermined inverse, that is, the variables number is greater than the equations number. This is because the collected data frequently do not give the complex mechanism explanation in the human body. Thanks to mathematical modeling, we would simulate complex activities and gain precious insight into in vivo pharmacokinetics. In [1] and [2], the authors proposed to apply the CNM in order to concomitantly seek many solutions for an undetermined inverse problem. Because the proposed CNM uses a least squares approach to collectively fit the Jacobian, it is more effective than algorithms that calculate many solutions one at a time. The CNM works by concurrently computing a cluster of solutions. It is proven that, the CNM is trustworthy, powerful, and efficient than the Levenberg-Marquardt method. In order to identify solutions family that best fits the additional requirements, in [3], the authors suggest a novel algorithm based on the Beta distribution's two parameters. As a result, it is possible to have considerably more control over the range of possible solutions when using the CNM. Additionally, the authors add

The associate editor coordinating the review of this manuscript and approving it for publication was Wentao Fan.

certain enhancements to the original CNM, such an error adaptive margin for the target value perturbation and an analytical Jacobian to the forward issue resolution.

In this work, we suggest two enhanced schemes for the CNM method. In the physiologically based pharmacokinetics (PBPK) problem, we need to find many points at the same time, hence the number of function evaluations will be very large (the CNM requests only one function evaluation/point/iteration). Therefore, in this study, we are interested in solutions that increase the computational efficiency for the CNM method through numerical treatment to reduce the number of iterations. It can be seen that the backslash operator fits quite well with the hyperplane in Step 2.2 of the original CNM [1], [2], [3], however, the stability still needs to be enhanced in view of the fact that (i) Stability deficiency of the solution with the meaning that parameter recognition is a hypothetical inverse problem. Especially, it can be greatly amplified by modeling error and measurement noise. By using the regularization approach, these issues can be solved. More specifically, the data mismatch minimization problem and the regularization issue could be considered as parameters of stable identification; (ii) Thanks to the single values contribution in the matrix operator, the quadratic filter behaves like the Tikhonov regularization. This filter can efficaciously dismiss singular values of order lower than those of normal parameters that leads to instability of matrix equations. For that reason, we propose to use Tikhonov regularization to handle the overdetermined system for hyperplane fitting in Step 2.2 in the early CNM. Tikhonov regularization has been also applied in many medical optimization problems, such as in B-mode imaging [4], [5], [6], X-ray imaging [7], [8], [9], ultrasound tomography [10], [11], MRI [12], [13], [14]. Besides a machine-learning based method in geophysics is also proposed to perform the inversion using direct mapping the seismic prestack data to seafloor elastic parameters [15]. To the best of our knowledge, Tikhonov has been used to solve inverse problems in many areas, including pharmacokinetics [16]. However, PBPK using cluster Newton method (CNM) to search for many solutions simultaneously, Tikhonov's regularization has not been considered.

In the early CNM, the PoC tends to inch closer to the SoM N* after each iteration. We must introduce randomly changing object values of h* (the amount of the current perturbation is 10%) [2] in order to ensure that the least squares issue is properly stated. Following every iteration, although the PoC tends to go closer to the SoM N*, the perturbation level will stay the same. Keeping this level of perturbation constant can introduce significant errors, especially as the point cluster is nearby the SoM. Therefore, we suggest a meaningful iterative manner in the CNM to determine the inverse parameter in pharmacokinetics. Following every iteration, as the PoC proceeds toward the N* solution path, and the noise reduction of h* needs to be implemented and this is suitable in numerical stabilization. Therefore, Stage 1 is divided into two sub-Stages (e.g., Stage 1 and Stage 2). Substage1 is executed with the use of a large h* disturbance for the first several iterations; Substage2 is executed with the use of a small h* disturbance for subsequent iterations. With this approach, the simulation results show that the moving the PoC is more stable, both the iterations number and the computed time are reduced. This solution is even better than Tikhonov regularization.

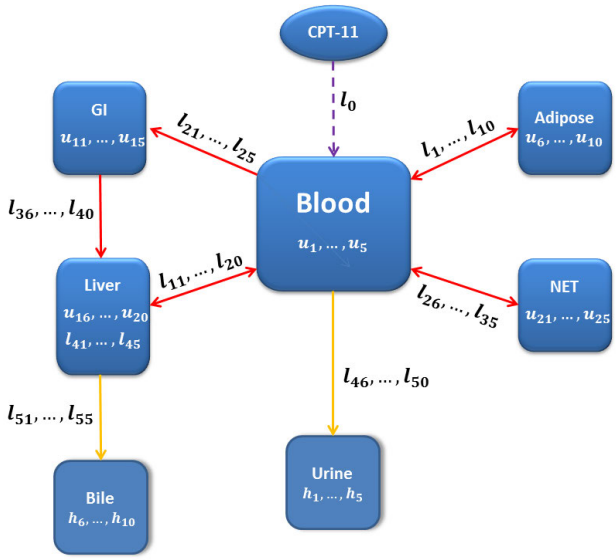

FIGURE 1. PBPK's simple diagram.

This paper is organized as follows. Section II describes physiologically based pharmacokinetics (PBPK), including forward problem: pharmacokinetics model; inverse problem: identification of model parameters; model problem representation. Section III describes early cluster newton method (CNM) for solving the underdetermined inverse problem. Section IV present the first proposed approach: Tikhonov regularization is used to fit a hyperplane for the CNM. Section V presents the second proposed approach: A CNM effective iteration procedure. Section VI present numerical experiments and results of two approaches. Finally, Section VII presents our conclusions. In this work, we have proposed two contributions, Tikhonov regularization and perturbation-level tuning, aiming to improve the traditional CNM method by increasing the convergence speed (i.e., reducing the relative error residual) and reducing the computational cost.

II. PHYSIOLOGICALLY BASED PHARMACOKINETICS (PBPK)

The PBPK provides a mathematical modelling method for predicting the absorption, distribution, metabolism, and excretion of the CPT-11 drug in human body. It is employed in pharmaceutical research and medication development, as well as in the evaluation of the health risks associated with chemicals. In this section, we present the forward problem from injecting CPT-11 into the body, then the inverse problem based on the excretion paths in urine and bile, and finally present the problem model of the PBPK.

A. FORWARD PROBLEM OF THE PBPK

In the beginning, through intravenous, the CPT-11 drug is injected into a person's body. The drug, denoted as $u_1(t), \ldots, u_{25}(t)$, along with its metabolites, which are SN-38, SN-38G, NPC, and APC, are modeled in each piece of the body, consisting blood, adipose, GI, liver and NET, based on the Arikuma's PBPK model [17]. Any chemical combination in every section is related via paths, $l_1, \ldots, l_{55}$, that show chemical compound inflow and outflow. Because the concentration variations are caused by the flow of chemical components, a concentrations system of the 1st order ordinary differential equation (ODE) indicated by $u_i(t)$ can be constructed as a time's function, t.

The pathways, depicted in Figure 1 as $l_1, \ldots, l_{55}$, have been modeled by Arikuma et al. Blood flow, metabolic, excretion, and i.v drip are the four types of routes that are taken into consideration. Every pathway provides a quantitative depiction of the drug flow rate. Regarding to these pathways, 60 parameters (typical values) denoted as $n_1, \ldots, n_{60}$ are shown in Table B1-B5 in [17]. This inverse problem purpose is to evaluate this model's parameters which are better than the representative values of clinical observation data listed in the table.

As $u_1(t), \ldots, u_{25}(t)$ are the CPT-11 concentrations along with its metabolics in parts. The concentration variations $\frac{du_i}{dt}$ are by the drug inflow and outflow with pathways. Hence, an ODE system can be constructed in order to represent for concentrations, $u_i(t)$, as follows:

$$\frac{d}{dt}u = h(u, t; n)$$

Detailed equations are expressed in the next page.

This is the 1st order ODE system, the ODE15s function in Matlab is used to resolve [20]. After that, u(n_1, …, n_{60}; t) can be obtained, they depend on variables, t and $n_1, \ldots, n_{60}$. Therefore, $u_1(t), \ldots, u_{25}(t)$ could be evaluated.

B. INVERSE PROBLEM: IDENTIFICATION OF MODEL PARAMETERS

In the inverse problem, with the outcomes of excretion pathways in urine as well as bile ($h \in R^{10}$), and a function of PBPK model ($f : R^{60} \to R^{10}$), PBPK's parameters as enzyme reaction speed, blood flow rate, and tissue volume, etc. ($n \in R^{60}$) are needed to estimate. The inverse problem model has been shown as follows:

$$h = f(n)$$

When formulated in vector form, it becomes:

$$\begin{aligned}&[h_1, h_2, \ldots, h_{10}]^T\\ &= [u_{26}(n_1, \ldots, n_{60}; T), \ldots, u_{35}(n_1, \ldots, n_{60}; T)]^T\\ &= [f_1(n_1, \ldots, n_{60}), \ldots, f_{10}(n_1, \ldots, n_{60})]^T\end{aligned}$$

where

$$\begin{cases} f_1(n) = u_{26}(n; T) = \int_0^T l_{46} = \int_0^T n_{26}.n_{21}.u_1(t)\,dt \\ f_2(n) = u_{27}(n; T) = \int_0^T l_{47} = \int_0^T n_{27}.n_{22}.u_2(t)\,dt \\ f_3(n) = u_{28}(n; T) = \int_0^T l_{48} = \int_0^T n_{28}.n_{23}.u_3(t)\,dt \\ f_4(n) = u_{29}(n; T) = \int_0^T l_{49} = \int_0^T n_{29}.n_{24}.u_4(t)\,dt \\ f_5(n) = u_{30}(n; T) = \int_0^T l_{50} = \int_0^T n_{30}.n_{25}.u_5(t)\,dt \\ f_6(n) = u_{31}(n; T) = \int_0^T l_{51} = \int_0^T (n_{31}.n_{21})/n_{11}.u_{16}(t)\,dt \\ f_7(n) = u_{32}(n; T) = \int_0^T l_{52} = \int_0^T (n_{32}.n_{22})/n_{12}.u_{17}(t)\,dt \\ f_8(n) = u_{33}(n; T) = \int_0^T l_{53} = \int_0^T (n_{33}.n_{23})/n_{13}.u_{18}(t)\,dt \\ f_9(n) = u_{34}(n; T) = \int_0^T l_{54} = \int_0^T (n_{34}.n_{24})/n_{14}.u_{19}(t)\,dt \\ f_{10}(n) = u_{35}(n; T) = \int_0^T l_{55} = \int_0^T (n_{35}.n_{25})/n_{15}.u_{20}(t)\,dt \end{cases}$$

In this inverse problem, it is characterized as an ordinary differential equation (ODE) system coefficient determination issue. The ODE system is used to simulate the transport and metabolism of the CPT-11 anticancer medication along with its metabolites. Noting that $u_i(t)\,(i = 1, 2, \ldots, 25)$ are all dependent on $n_i (i = 1, 2, \ldots, 60)$, and a mapping function from the n_i to the excretion paths $h_i (i = 1, 2, \ldots, 10)$ may be found. That is, the connection among parameters (unknown) and output data (observable) is known with the PBPK model. When this inverse problem is solved, patient's multiple feasible biological states consistent with the clinical observations can be found.

C. MODEL PROBLEM REPRESENTATION

The PBPK's model parameter identifying problem is identified as: Seek points set in $N \subset R^{60}$ near a box N^0, that satisfies:

$$h^* = f(n)$$

in which

$f : N \subset R^{60} \to R^{10}$: a mapped function.

h^* : Patient's clinical output.

$$N = \left\{ n \in R^{60} : n_i > 0 v\grave{a} \sum\nolimits_{i=55}^{58} n_i < 1000 \right\}$$

$$N^0 = \left\{ n \in R^{60} : \max_{i=1,2,\ldots,60} \left| \frac{n_i - \widehat{n_i}}{\widehat{n_i} v_i} < 1 \right| \right\}$$

The representative values of model parameters are extracted in the work of Arikuma [17] and these values are symbolized as $\widehat{n_i} (i = 1, 2, \ldots, 60)$. The kinetic parameter variability and physiological parameters are chosen according to the works [22], [23] (the variation is ±50% for kinetic parameters, ±30% for physiological parameters, and ±5% for drug administration parameters). The i.v drip infusion parameter variability is sized to be compact since it just influenced by the drip infusion process accuracy.

III. EARLY CLUSTER NEWTON METHOD (CNM)

Because the presented schemes are only relevant to the CNM's Stage 1 (the leading stage), hence, just the first stage of the CNM is discussed in this section:

$$
\begin{cases}
\frac{d}{dt}u_1 = \left(\frac{n_{59}}{n_{60}} + \frac{n_{51}}{n_1}.u_6(t) + \frac{(n_{52}+n_{53})}{n_{11}}.u_{16}(t) + \frac{n_{54}}{n_{16}}.u_{21}(t) - n_{51}.u_1(t) - n_{53}.u_1(t) - n_{52}.u_1(t) - n_{54}.u_1(t) \right. \\
\qquad \left. - n_{26}.n_{21}.u_1(t)\right)/n_{55} \\
\frac{d}{dt}u_2 = \left(\frac{n_{51}}{n_2}.u_7(t) + \frac{(n_{52}+n_{53})}{n_{12}}.u_{17}(t) + \frac{n_{54}}{n_{17}}.u_{22}(t) - n_{51}.u_2(t) - n_{53}.u_2(t) - n_{52}.u_2(t) - n_{54}.u_2(t) \right. \\
\qquad \left. - n_{27}.n_{22}.u_2(t)\right)/n_{55} \\
\frac{d}{dt}u_3 = \left(\frac{n_{51}}{n_3}.u_8(t) + \frac{(n_{52}+n_{53})}{n_{13}} + \frac{n_{54}}{n_{18}}.u_{23}(t) - n_{51}.u_3(t) - n_{53}.u_3(t) - n_{52}.u_3(t) - n_{54}.u_3(t) - n_{28}.n_{23}.u_3(t)\right)/n_{55} \\
\frac{d}{dt}u_4 = \left(\frac{n_{51}}{n_4}.u_9(t) + \frac{(n_{52}+n_{53})}{n_{14}}.u_{19}(t) + \frac{n_{54}}{n_{19}}.u_{24}(t) - n_{51}.u_4(t) - n_{53}.u_4(t) - n_{52}.u_4(t) - n_{54}.u_4(t) \right. \\
\qquad \left. - n_{29}.n_{24}.u_4(t)\right)/n_{55} \\
\frac{d}{dt}u_5 = \left(\frac{n_{51}}{n_5}.u_{10}(t) + \frac{(n_{52}+n_{53})}{n_{15}}.u_{20}(t) + \frac{n_{54}}{n_{20}}.u_{25}(t) - n_{51}.u_5(t) - n_{53}.u_5(t) - n_{52}.u_5(t) - n_{54}.u_5(t) \right. \\
\qquad \left. - n_{30}.n_{25}.u_5(t)\right)/n_{55} \\
\frac{d}{dt}u_6 = \left(n_{51}.u_1(t) - l_1 = \frac{n_{51}}{n_1}.u_6(t)\right)/(1000 - n_{55} - n_{56} - n_{57} - n_{58}) \\
\frac{d}{dt}u_7 = \left(n_{51}.u_2(t) - \frac{n_{51}}{n_2}.u_7(t)\right)/(1000 - n_{55} - n_{56} - n_{57} - n_{58}) \\
\frac{d}{dt}u_8 = \left(n_{51}.u_3(t) - \frac{n_{51}}{n_3}.u_8(t)\right)/(1000 - n_{55} - n_{56} - n_{57} - n_{58}) \\
\frac{d}{dt}u_9 = \left(n_{51}.u_4(t) - \frac{n_{51}}{n_4}.u_9(t)\right)/(1000 - n_{55} - n_{56} - n_{57} - n_{58}) \\
\frac{d}{dt}u_{10} = \left(n_{51}.u_5(t) - \frac{n_{51}}{n_5}.u_{10}(t)\right)/(1000 - n_{55} - n_{56} - n_{57} - n_{58}) \\
\frac{d}{dt}u_{11} = \left(n_{52}.u_1(t) - \frac{n_{51}}{n_6}.u_{11}(t)\right)/n_{56};\ \frac{d}{dt}u_{12} = \left(n_{52}.u_2(t) - \frac{n_{51}}{n_7}.u_{12}(t)\right)/n_{56} \\
\frac{d}{dt}u_{13} = \left(n_{52}.u_3(t) - \frac{n_{51}}{n_8}.u_{13}(t)\right)/n_{56};\ \frac{d}{dt}u_{14} = \left(n_{52}.u_4(t) - \frac{n_{51}}{n_9}.u_{14}(t)\right)/n_{56} \\
\frac{d}{dt}u_{15} = \left(n_{52}.u_5(t) - \frac{n_{51}}{n_{10}}.u_{15}(t)\right)/n_{56} \\
\frac{d}{dt}u_{16} = \left(n_{53}.u_1(t) + \frac{n_{51}}{n_6}.u_{11}(t) - \frac{(n_{52}+n_{53})}{n_{11}}.u_{16}(t) - \frac{n_{41}.n_{46}.n_{57}}{\frac{n_{36}.n_{11}}{n_{21}.u_{16}(t)}+1} - \frac{n_{44}.n_{49}.n_{57}}{\frac{n_{39}.n_{11}}{n_{21}.u_{16}(t)}+1} \right. \\
\qquad \left. - \frac{n_{43}.n_{48}.n_{57}}{\frac{n_{38}.n_{11}}{n_{21}.u_{16}(t)}+1} - \frac{n_{31}.n_{21}}{n_{11}}.u_{16}(t)\right)/n_{57} \\
\frac{d}{dt}u_{17} = \left(n_{53}.u_2(t) + \frac{n_{51}}{n_7}.u_{12}(t) + \frac{n_{41}.n_{46}.n_{57}}{\frac{n_{36}.n_{11}}{n_{21}.u_{16}(t)}+1} + \frac{n_{42}.n_{47}.n_{57}}{\frac{n_{37}.n_{14}}{n_{24}.u_{19}(t)}+1} - \frac{(n_{52}+n_{53})}{n_{12}}.u_{17}(t) \right. \\
\qquad \left. - \frac{n_{45}.n_{50}.n_{57}}{\frac{n_{40}.n_{12}}{n_{22}.u_{17}(t)}+1} - \frac{n_{32}.n_{22}}{n_{12}}.u_{17}(t)\right)/n_{57} \\
\frac{d}{dt}u_{18} = \left(n_{53}.u_3(t) + \frac{n_{51}}{n_8}.u_{13}(t) + \frac{n_{45}.n_{50}.n_{57}}{\frac{n_{40}.n_{12}}{n_{22}.u_{17}(t)}+1} - \frac{(n_{52}+n_{53})}{n_{13}}.u_{18}(t) - \frac{n_{33}.n_{23}}{n_{13}}.u_{18}(t)\right)/n_{57} \\
\frac{d}{dt}u_{19} = \left(n_{53}.u_4(t) + \frac{n_{51}}{n_9}.u_{14}(t) + \frac{n_{44}.n_{49}.n_{57}}{\frac{n_{39}.n_{11}}{n_{21}.u_{16}(t)}+1} - \frac{(n_{52}+n_{53})}{n_{14}}.u_{19}(t) - \frac{n_{42}.n_{47}.n_{57}}{\frac{n_{37}.n_{14}}{n_{24}.u_{19}(t)}+1} - \frac{n_{34}.n_{24}}{n_{14}}.u_{19}(t)\right)/n_{57} \\
\frac{d}{dt}u_{20} = \left(n_{53}.u_5(t) + \frac{n_{51}}{n_{10}}.u_{15}(t) + \frac{n_{43}.n_{48}.n_{57}}{\frac{n_{38}.n_{11}}{n_{21}.u_{16}(t)}+1} - \frac{(n_{52}+n_{53})}{n_{15}}.u_{20}(t) - \frac{n_{35}.n_{25}}{n_{15}}.u_{20}(t)\right)/n_{57} \\
\frac{d}{dt}u_{21} = \left(n_{54}.u_1(t) - \frac{n_{54}}{n_{16}}.u_{21}(t)\right)/n_{58};\ \frac{d}{dt}u_{22} = \left(n_{54}.u_2(t) - \frac{n_{54}}{n_{17}}.u_{22}(t)\right)/n_{58} \\
\frac{d}{dt}u_{23} = \left(n_{54}.u_3(t) - \frac{n_{54}}{n_{18}}.u_{23}(t)\right)/n_{58};\ \frac{d}{d??}u_{24} = \left(n_{54}.u_4(t) - \frac{n_{54}}{n_{19}}.u_{24}(t)\right)/n_{58} \\
\frac{d}{dt}u_{25} = \left(n_{54}.u_5(t) - \frac{n_{54}}{n_{20}}.u_{25}(t)\right)/n_{58}
\end{cases}
$$

1: Set the initial values and starting positions for the objects.

1-1: Choose starting points at random $\left\{n_{.j}^{(0)}\right\}_{j=1}^{l}$ in the N^0 box. They are preserved in a $N^{(0)}$ matrix of the $60\times l$ size with each column corresponding to a $n_{.j}$ point in R^{60}.

1-2: To guarantee that step 2-2 is well-posed, generate randomly disturbed object values $\left\{h_j^*\right\}_{j=1}^{l}$ near h*. The values of $h_{.j}^*$ is selected as follows:

$$\max_{i=1,2,\ldots,10}\left|\frac{h_{ij}^*-h_i^*}{h_i^*}\right|<\eta$$

where $\eta = 0.1$ indicating the ifirst stage target accuracy ($\pm 10\%$). These vectors are collected in a H* matrix, with $h_{.j}^*$ in column j.

2: For k = 0, 1, 2, …, K_1

2-1: Deal with each point in $N^{(k)}$ in the forward problem as follows:

$$H^{(k)}=f(N^{(k)})$$

where the solution of the f function at every column of $N^{(k)}$ corresponds to each column of $H^{(k)}$.

2-2: Construct a linear approximation of f, it becomes:

$$f\ (n)\approx A^{(k)}n+h_0^{(k)}$$

via fitting a plane to the axis of $H^{(k)}$. The least squares approach of an overdetermined linear equations system [18] can be used to seek the slope matrix $A^{(k)}$ along with the shifting constant $h_0^{(k)}$:

$$\min_{A_{(k)}\in R^{10\times 60},h_o^{(k)}\in R^{10}}\left\|H^{(k)}-(A^{(k)}N^{(k)}+H_0^{(k)})\right\|_F$$

here $H_0^{(k)}$ is a matrix with the size of $10\times l$ whose columns are all $h_0^{(k)}$.

2-3: Using a linear approximation, detect the updating vector $s_{.j}^{(k)}$ for all columns of $N^{(k)}$, that is, seek $s_{.j}$ meets:

$$h_{.j}^*=A^{(k)}\left(n_{.j}^{(k)}+s_{.j}^{(k)}\right)+h_0^{(k)}\text{với } j=1,2,\ldots,l(*)\quad(1)$$

Matrix A has a rectangular form in which the number of columns is larger than that of rows, resulting in a linear equations system with an underdetermined solution. Hence, the unique determination of $s_{.j}^{(k)}$ that satisfies Equation (∗) cannot be solved. Of all the obtained solutions of Eq. (∗), the vector $s_{.j}^{(k)}$ is selected with the smallest scaling length. The vectors $\left\{s_{.j}^{(k)}\right\}_{j=1}^{l}$ are the solution of an underdetermined linear equations system that offers the minimum norm, given as a matrix $S^{(k)}$

$$\min_{S^{(k)}\in R^{60\times l}}\left\|diag\ (\widehat{n})^{-1}\ S^{(k)}\right\|_F$$
$$\text{subjectsto } H^*=(A^{(k)}(N^{(k)}+S^{(k)})+H_0^{(k)})$$

in which, $\widehat{n}=(\widehat{n_1},\widehat{n_2},\ldots,\widehat{n_{60}})$.

2-4: Using updating $N^{(k)}$, seek new points that resemble the N*SoM. If needed, the vector length $s_{.j}^{(k)}$ is shrinked until the point, $(n_{.j}^{(k)}+s_{.j}^{(k)})$, is inside the domain of the f function, as follows:

For $j=1,2,\ldots,l$

While $(n_j^{(k)}+s_j^{(k)})\notin X$

$$s_j^{(k)}=\frac{1}{2}s_{.j}^{(k)}$$

End while

End for

$$N^{(k+1)}=N^{(k)}+S^{(k)}$$

End for

To assess the algorithm accuracy, the relative error residual (RRE) is defined as:

$$r_j^{(k)}(n)=\max_{i=1,2,\ldots,10}\left|\frac{h_{ij}^{(k)}-h_i^*}{h_i^*}\right|\text{với}h_j^{(k)}=f(n_j^{(k)}).$$

The traditional CNM method can be summarized in the following six main steps:

1. Choose the starting points at random in box N^0.
2. Randomly generate perturbation target values close to h* to confirm that the least squares problem is properly well-posed.
3. Evaluate the function f for each N(k) point.
4. Build a plane-fitted linear approximation of f.
5. Find an approximate linear update vector $s_{.j}^{(k)}$ for each point.
6. Seek new points that approximate different solutions N* with updated $N^{(k)}$.

Our contributions expressed in the traditional CNM method are as follows: The first proposed solution (Tikhonov regularization) is applied in step 4 in the traditional CNM; The second proposed solution (perturbation-level tuning) is applied in step 2 in the traditional CNM.

IV. THE FIRST PROPOSED APPROACH: TIKHONOV REGULARIZATION IS USED TO FIT A HYPERPLANE FOR THE CNM

The second-order regularization (Tikhonov regularization) adds a regularization parameter and acts as a filter. It can filter out the oddly small values that cause instability in the system. The 2nd order regularization is suitable for sparse and dense data. In the case of using the first-order regularization, it is suitable for sparse data problems, whereas the number of point sets in the PBPK problem is huge, so it cannot be sparse; therefore, the first-order regularization is not suitable to apply to the problem of dense data points.

Tikhonov regularization overcomes the matrix inversion numerical instability and then offers lower variance models of solving *minimize* $\|y-Ax\|_2^2$. This scheme supplements a positive constant to the A^TA diagonals, to make the matrix nonsingular [19]. Tikhonov regularization has the form as:

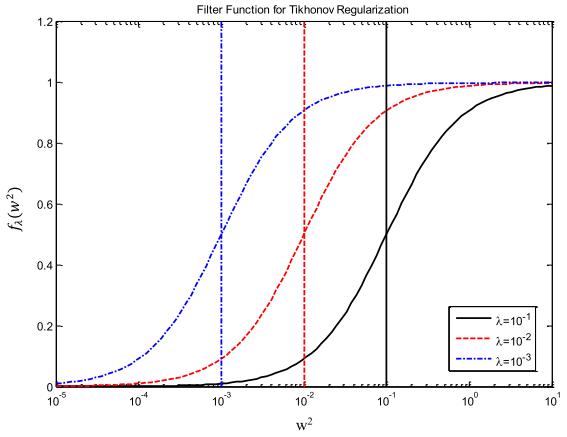

FIGURE 2. Tikhonov filter function.

minimize $F(x) = \text{minimize } \frac{1}{2}\|y - Ax\|_2^2 + \frac{\lambda}{2}\|x\|_2^2$ and we have the solution:

$$\leftrightarrow x = \left(A^T A + \lambda I\right)^{-1} \mathrm{A}^{\mathrm{T}} y(**)$$

In the form of SVD, assumed that a real $A_{m\times n}$ is full rank ($m \gg n$), $A = DWE^T$ in which D is orthogonal to E, $\mathrm{D} = [\mathrm{d}_1, \ldots, \mathrm{d}_\mathrm{m}) \in \mathrm{R}^{\mathrm{m}\times\mathrm{m}}$, $\mathrm{E} = [\mathrm{e}_1, \ldots, \mathrm{e}_\mathrm{n}) \in \mathrm{R}^{\mathrm{n}\times\mathrm{n}}$ and $\mathrm{W} = \mathrm{diag}(\mathrm{w}_1, \ldots, \mathrm{w}_\mathrm{n}) \in \mathrm{R}^{\mathrm{n}\times\mathrm{n}}$ where $\mathrm{w}_1 \geq \mathrm{w}_{2\geq} \ldots, \mathrm{w}_\mathrm{n} \geq 0$, w_i is the i-th singular value. From (**), we have the solution:

$$x = \sum\nolimits_{i=1}^{n} f_i \left(\frac{d_i^T y}{\mathrm{w_i}}\right) e_i$$

where $f_i = \frac{\mathrm{w_i^2}}{\mathrm{w_i^2}+\lambda}$ is referred to as a filter function of Tikhonov regularization.

The regularization parameter, λ, has the following effect of the filter function: a small value of λ is unaffected in a large value of $\mathrm{w_i}$ ($\lambda \ll \mathrm{w_i}$), i.e. $f_i = \frac{\mathrm{w_i^2}}{\mathrm{w_i^2}+\lambda} \approx \frac{\mathrm{w_i^2}}{\mathrm{w_i^2}} = 1$; a large value of λ can decrease the magnification of $1/\mathrm{w_i}$, because $f_i = \frac{\mathrm{w_i^2}}{\mathrm{w_i^2}+\lambda} \approx \frac{\mathrm{w_i^2}}{\lambda} \ll 1$.

Figure 2 shows Tikhonov filter function. Singular components which are small in comparison with λ are filtered out by Tikhonov regularization while retaining components that are large. Hence, on the singular values contribution of the matrix operator, second-order filtering is accomplished through Tikhonov regularization. The filtering result is to beneficially eliminate the singular values that are of a lower order than λ. These values are the cause for the matrix equation instability.

In short, a positive constant λ is added to every singular value $\mathrm{w_i^2}$ of $\mathrm{A^TA}$ by Tikhonov regularization. It can be considered as smoothing. Over smoothing is when we choose λ that is too high, while undersmoothing is when we choose λ that is too low. The benefactions of every vector e_i to the solution are reduced as a result of this smoothing. Therefore, a good selection of λ can offer enough numerical stability to obtain a good approximate solution.

In [21], Aoki specified that, solving $\min_{A_{(k)}\in R^{10\times 60}, h_o^{(k)}\in R^{10}} \left\|H^{(k)} - (A^{(k)}N^{(k)} + H_0^{(k)})\right\|_F$ is equivalent to *minimize* $\|y - Ax\|_2^2$. Hence, Tikhonov regularization in the presented scheme has the form *minimize* $\|y - Ax\|_2^2 + \lambda\|x\|_2^2$. In the form of SVD, the solution is $n = \sum_{i=1}^{n} f_i \left(\frac{d_i^T h}{\mathrm{w_i}}\right) e_i$.

V. THE SECOND PROPOSED APPROACH: A CNM EFFECTIVE ITERATION PROCEDURE

In this section, an effective CNM iteration approach for identifying inverse parameters in pharmacokinetics is provided. After each iteration in the first CNM, the PoC tends to grow closer to the SoM, N*. To make sure that the least squares problem is well-posed, we are required to induce randomly altered object values of h* (the present level of perturbation is 10%). Although the PoC move closer to the SoM N* with each iteration, the perturbation level remain same.

For the case that the PoC is separated from the N* SoM, the component values in the PoC diverge significantly from those of the SoM. Hence, a strong enough perturbation level is required to guarantee the well-posedness in the least squares issue by providing an essential difference among the components in the PoC as well as SoM.

For the case that the PoC is near to the N* SoM, the component values in the PoC are not considerably different from the ones in the SoM. Therefore, to guarantee the well-posedness in the least squares issue, we just need to produce a lower perturbation level which also presents a notable distinction between the components in the PoC as well as SoM.

As a result, decreasing the perturbation level of h* after every iteration, when the PoC is adjacent to the SoM N*, is necessary and acceptable for numerical stabilization. It signifies that Stage 1 is split into two halves (i.e., Substage1 and Substage2). For the first few iterations, we use a big perturbation level of h*, and for the remainder of the iterations, we use a minor perturbation level of h*. Numerical simulation results show that with this proposed scheme, the PoC move more stably, the iteration number and computation time can be saved. This approach is even more superior than the implementation of Tikhonov regularization.

VI. NUMERICAL EXPERIMENTS AND RESULTS

Numerical simulation parameters of the first suggested scheme: Sample number $\mathrm{N_{samp}} = 500$, total iteration number $\mathrm{N_{iter}} = 10$, function evaluation accuracy $\delta_{ODE} = 10^{-3}$, regularization parameter $\lambda = 10^{-12}$, perturbation level 10%.

Numerical simulation parameters of the second suggested scheme: Sample number $\mathrm{N_{samp}} = 500$, total iteration number $\mathrm{N_{iter}} = 10$, the first Substage's iteration number $\mathrm{N_{1-iter}} = 2$, the second Substage's iteration number $\mathrm{N_{1-iter}} = 8$, function evaluation accuracy $\delta_{ODE} = 10^{-3}$, the first stage's perturbation level 10%, the second stage's perturbation level 6%. The computational cost of the iterative algorithm depends on the number of iterations ($\mathrm{N_{iter}}$) and the number of points in

TABLE 1. RRE of the early CNM and suggested approaches.

Methods	RRE after every iteration (1-10)										Runtime (sec)
The early CNM	**3.1452**	**0.8131**	**0.5434**	**0.2516**	**0.1401**	**0.1324**	**0.1200**	0.1155	0.1124	0.1115	461.882349
The first approach	**3.1452**	**0.8214**	**0.5170**	**0.1990**	**0.1430**	0.1182	0.1126	0.1132	0.1123	0.1133	416.989932
The second approach	**3.1452**	**0.8054**	**0.5270**	**0.1871**	**0.1268**	0.1154	0.1111	0.1064	0.1049	0.1036	417.197260

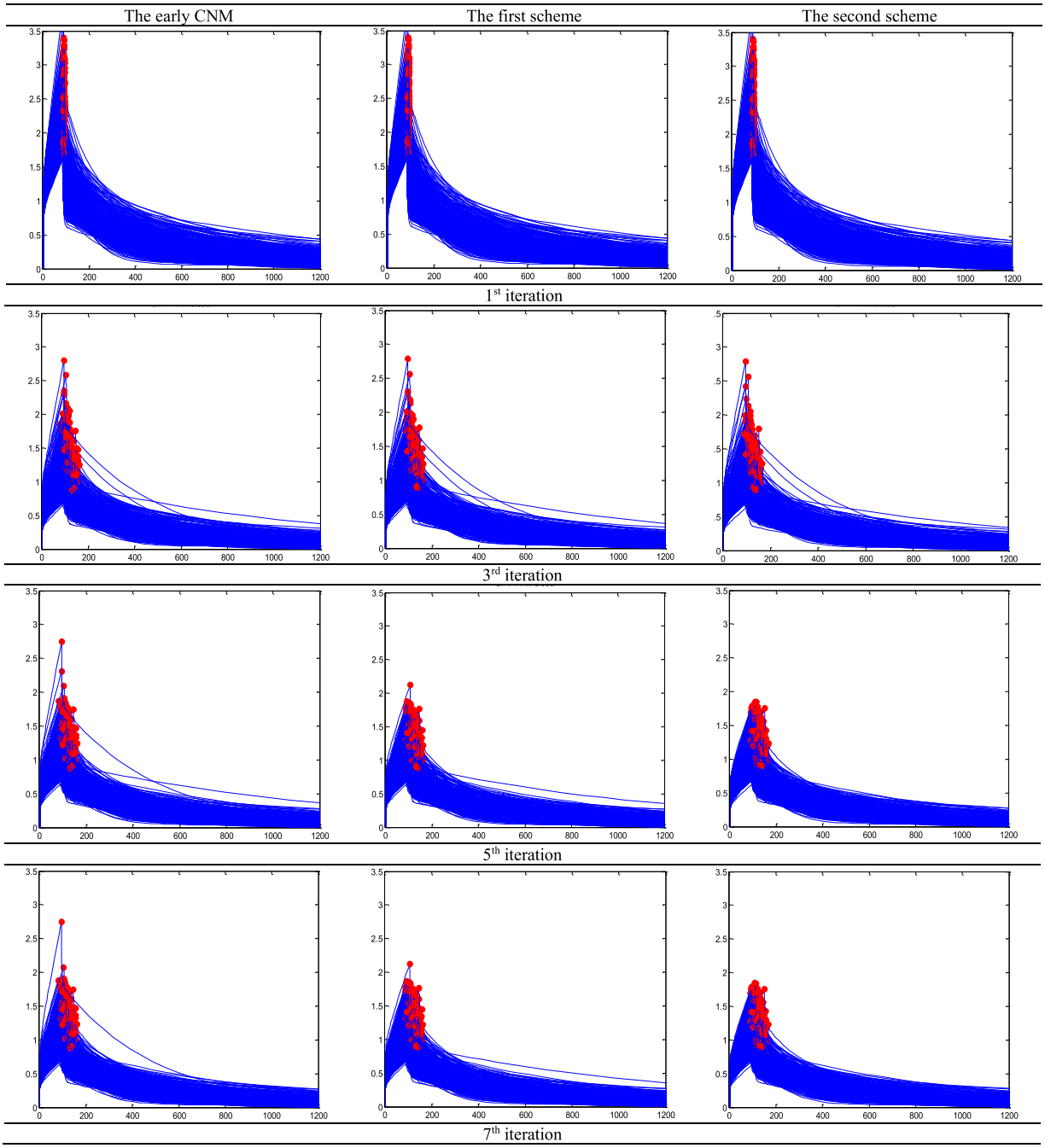

FIGURE 3. The CPT-11 content in blood was predicted utilizing 500 sets of samples obtained by the early CNM, as well as proposed techniques. The vertical axis expresses concentration of CPT-11 in blood (μmol/L), and horizontal axis expresses time elapsed (minutes).

the cluster of points (N_{samp}). Therefore, the computational cost is denoted by $O(N_{iter} \times N_{samp})$. We used the PBPK model code package produced by Arikuma irinotecan and Yasunori Aoki, specifically as follows: Takeshi Arikuma created the

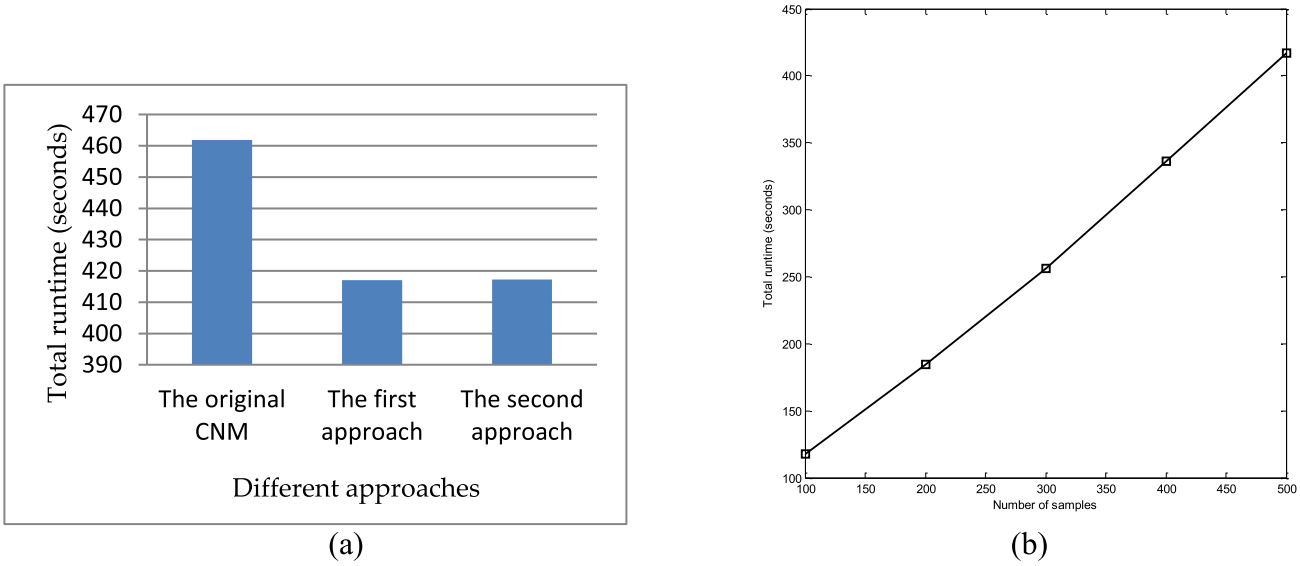

FIGURE 4. (a) The calculated total runtime of the original CNM and two proposed approaches and (b) Influence of total runtime on different numbers of samples obtained by the CNM effective iteration procedure.

Arikuma irinotecan PBPK model in GNU Octave in 2008, and Yasunori Aoki enhanced it in Matlab in 2011.

In the solution using the Tikhonov filter, the algorithm will converge faster due to the use of the Tikhonov filter function. In the noise level turning solution, when the cluster of points approaches the target, the noise level should also be reduced for a better target approach and thus increase the convergence speed. In our problem, we compare the original CNM algorithm in the finite number of steps through the relative error residual (RRE).

To get out of the loop, there are two solutions: set a fixed number of loops or set a target error. The iterative algorithm will be excited when one of the above two criteria is satisfied. In our problem, we set a fixed number of iterations of 10; the algorithm will end after ten iterations. Our objective is to observe the normalization error and cluster migration after the first ten iterations between the traditional CNM method and the proposed solutions. The numerical simulation results indicate that the two proposed solutions converge quicker than the standard CNM. In our work, we applied Tikhonov regularization and perturbation-level tuning with the aim of improving the traditional CNM method by increasing the convergence speed (i.e., reducing RRE) and reducing the computational cost. We have only analyzed RRE reduction and computation cost.

Table 1 shows the RRE solved by early CNM and the suggested schemes after N_{sum} iterations. It is clearly that, the smallest RRE (RRE_{min}) in Stage 1 that the algorithm can obtain is 0.11, i.e., 11%. Evidently, seven iterations are needed in the early CNM for achieving RRE_{min}, while five iterations are just needed in the proposed approaches. As a result, at this stage, two iterations can be saved. That is, 1000 function evaluations can be saved. This is the cause that the CNM requests evaluation of only one

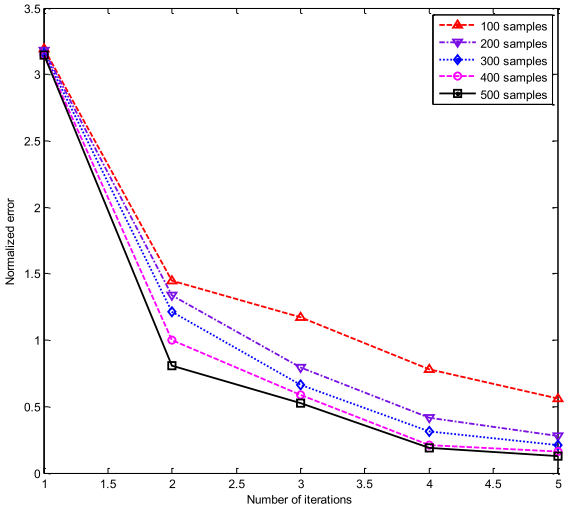

FIGURE 5. Investigation of normalized error corresponding to different numbers of samples obtained by the CNM effective iteration procedure.

function/point/iteration, so with 500 points and two iterations, there are 1000 function assessments. As a matter of fact, multiple feasible solutions need to be found, causing a great samples number which is greater than 1,000. Consequently, iteration save is noteworthy because it can decrease the CNM's computational complexity.

Additionally, for the equal amount of iterations of ten, the computed time of the suggested strategy is also considerably lessened, the computed time of the first suggested scheme and the early CNM are 416.989932 and 461.882349 seconds, respectively, that is the computed time decreased by 9.76% after 10 iterations (see Table 1 and Figure 4a). In the fact that, the suggested schemes require only five iterations (the early CNM needs seven iterations), the implementation time of the

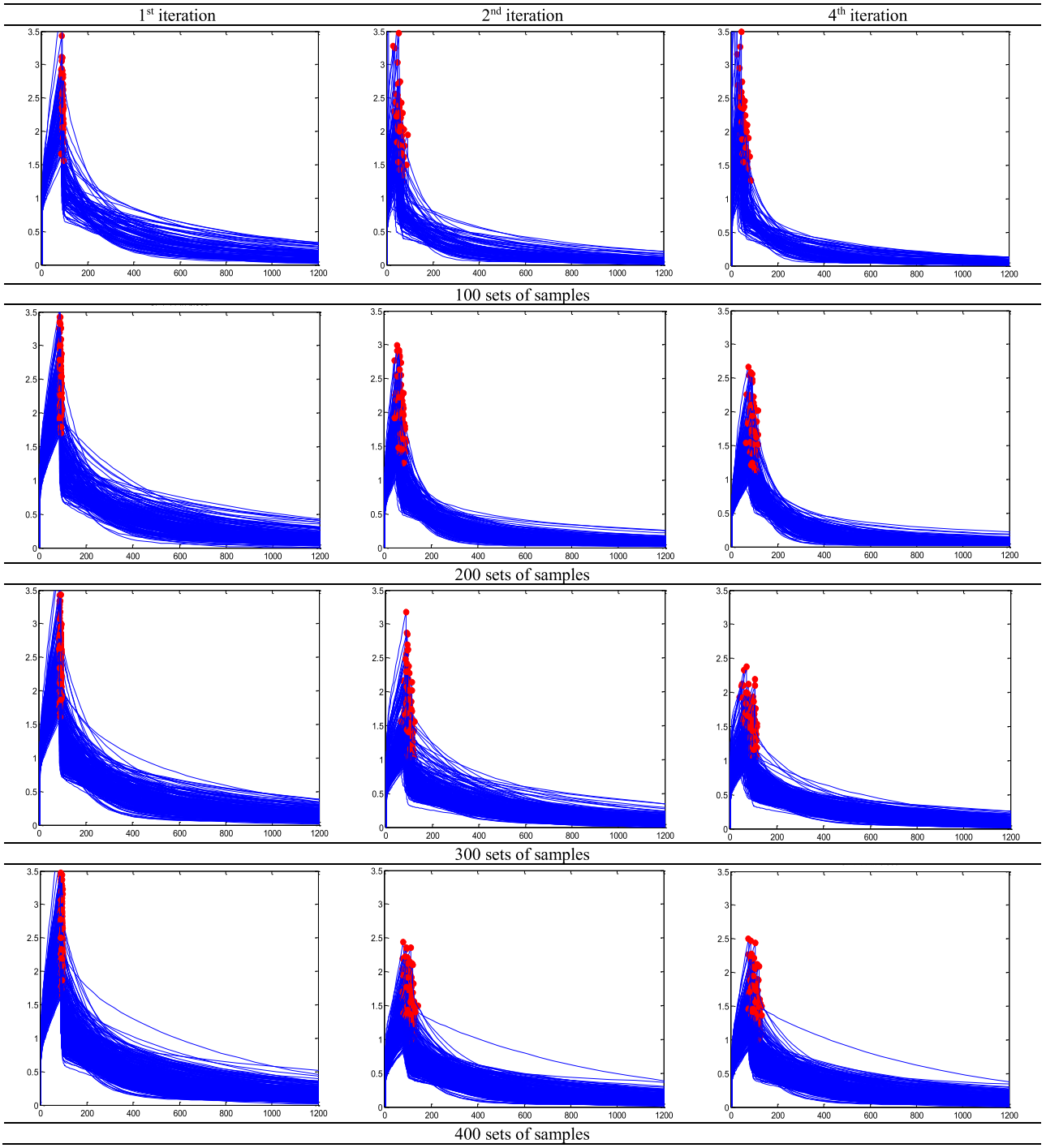

FIGURE 6. The CPT-11 content in blood was predicted utilizing 100, 200, 300, and 400 sets of samples obtained by the CNM effective iteration procedure in the first, second, and third iterations, respectively. The vertical axis expresses concentration of CPT-11 in blood (μmol/L), and horizontal axis expresses time elapsed (minutes).

suggested schemes decreases much more. With the identical iteration number, we can explain the reduced computation time of the first suggested scheme because the Tikhonov filter function may filter out tiny singular components in comparison with λ, therefore these values are not included in the calculation implementation. Meanwhile the early CNM still computes these values, the computation time will increase.

Figure 3 depicts the CPT-11 concentration projected findings in blood with the use of 500 parameter sets derived from the original CNM and suggested schemes. The blue lines show how drug concentrations change over time. As the drug is introduced into the body and begins to be metabolized, the drug's concentration is rising. The medication concentration eventually reaches a point when it stops rising and starts to fall. The red dot represents the maximum drug concentration.

Based on the observations, the difference between the early CNM and suggested schemes is not visible after the first and third repetitions. A significant difference between the early CNM and suggested schemes could be noticed after the fifth and seventh iterators, the PoC of the suggested schemes moved more steadily towards the SoM. Meanwhile, several samples are still distributed far from the PoC center in the early CNM. As a result of the Tikhonov regularization's nature and a CNM effective iteration procedure, we may be able to obtain a more stable and sensible solution.

Figure 4 presents the calculated total runtime comparison of the original CNM and two proposed approaches (Figure 4a) and the influence of total runtime on different numbers of samples obtained by the CNM effective iteration procedure (Figure 4b). We see that, as the number of samples increases from 100 to 500, so does the total runtime. This is reasonable because with the fixed number of iterations, the number of function evaluations will increase with the number of samples, so the function evaluation time will increase. Figure 5 presents the investigation of normalized error corresponding to different numbers of samples (100, 200, 300, 400, and 500) obtained by the CNM effective iteration procedure approach. As the number of iterations increases, the normalized error decreases. This is reasonable because during hyperplane fitting, The collection of points shifts gradually to the manifold of solutions with the greater number of iterations. And in the case when the number of samples increases, the normalized error decreases, this is because the larger the number of points, the easier it is to fit the hyperplane in the CNM method, and thus the cluster of points will focus and move more convenient to the manifold of solutions. This is also observed in Figure 6, especially when the amount of iterations grows (the fourth iteration from 100 to 400 number of samples). Some limitations that we need to further improve are constructing a practical method for determining regularization parameters appropriate for the CNM, determining the most efficient method for producing h^* perturbation and the number of investigated samples need much more to meet actual problem.

Because the information we clinically gather from living patients through treatment is often much less than the complexity of the inner workings of the patient, the inverse problem often arises in the area of medicine-mathematics. The fact that, the inspiration for our attentiveness in the uncertainty inverse problem was derived from the problem of determining the parameters of the pharmacokinetic model for CPT-11, a cancer treatment medication (also known as Irinotecan). Konagaya offered a work ''virtual patient population convergence'' [24], where the main idea is to estimate the parameters of a pharmacokinetic model in the whole body, based on observational data clinical patient. The main distinction of this work with parameter-defined solutions is that, as opposed to looking for a single set of parameters that fit the pharmacokinetic model to reconstruct clinical observation data, its purpose is to seek many sets of such parameters. The purpose of identifying these various parameter sets was to take into account the various potential effects of drug kinetics in the patient's body.

VII. CONCLUSION

In this study, based on the early cluster Newton method, we propose two approaches to enhance the quality of finding many possible point sets in solving the underdetermined inverse problem of the physiologically based pharmacokinetics. Tikhonov regularization was effectively used to fit a hyperplane, and an effective CNM iteration approach was considered to beneficially tune the perturbation level for warranting the well-posed least squares issue, in the early CNM for identifying inverse parameters in the field of pharmacokinetics. Therefore, we may (i) lessen number of iterations; (ii) lessen computing time; and (iii) the PoC progresses more steadily towards the SoM when using the proposed approaches. With the proposed approaches, in our numerical experiments, two iterations (that is 1000 function evaluations) can be saved and the computed time decreased by 9.76% after ten iterations in comparison with the early CNM. With the gained results, we need to further improve some issues such as (a) develop an effective scheme for calculating regularization parameter which is suited for the CNM; (b) how to identify the best percent of generating perturbation of h^*.

ACKNOWLEDGMENT

Prof. Ken Hayami and Dr. Yasunori Aoki of the National Institute of Informatics introduced them to pharmacokinetics, which the authors gratefully acknowledge.

REFERENCES

[1] Y. Aoki, K. Hayami, H. De Sterck, and A. Konagaya, ''Cluster newton method for sampling multiple solutions of an underdetermined inverse problem: Parameter identification for pharmacokinetics,'' Nat. Inst. Inform., Tokyo, Japan, NII Tech. Rep., 2011.

[2] Y. Aoki, K. Hayami, H. D. Sterck, and A. Konagaya, ''Cluster Newton method for sampling multiple solutions of underdetermined inverse problems: Application to a parameter identification problem in pharmacokinetics,'' *SIAM J. Sci. Comput.*, vol. 36, no. 1, pp. B14–B44, Jan. 2014.

[3] P. Gaudreau, K. Hayami, Y. Aoki, H. Safouhi, and A. Konagaya, ''Improvements to the cluster Newton method for underdetermined inverse problems,'' *J. Comput. Appl. Math.*, vol. 283, pp. 122–141, Aug. 2015.

[4] Y. Wang, F. Dong, and S. Ren, ''B-mode ultrasound images guided electrical impedance tomography image reconstruction via cross gradient,'' in *Proc. IEEE Int. Instrum. Meas. Technol. Conf. (I2MTC)*, May 2021, pp. 1–6.

[5] J. Cunningham, Y. Zheng, T. Subramanian, and M. Almekkawy, ''Regularization methods for solving third-order Volterra filter with improved convergence speed: In-vivo application,'' in *Proc. IEEE 15th Int. Symp. Biomed. Imag.*, Apr. 2018, pp. 1187–1190.

[6] P. Stahli, M. Frenz, and M. Jaeger, ''Bayesian approach for a robust speed-of-sound reconstruction using pulse-echo ultrasound,'' *IEEE Trans. Med. Imag.*, vol. 40, no. 2, pp. 457–467, Feb. 2021.

[7] A. Jardin, J. Bielecki, D. Mazon, Y. Peysson, K. Król, D. Dworak, and M. Scholz, ''Implementing an X-ray tomography method for fusion devices,'' *Eur. Phys. J. Plus*, vol. 136, no. 7, pp. 1–30, Jul. 2021.

[8] H. Ogawa, S. Ono, Y. Watanabe, Y. Nishikawa, S. Nishitsuji, T. Kabe, and M. Takenaka, ''Artifact removal in the contour areas of SAXS-CT images by Tikhonov-L1 minimization,'' *J. Appl. Crystallogr.*, vol. 54, no. 6, pp. 1784–1792, Dec. 2021.

[9] J. Xiang, S. Takeda, Y. Cai, H. Tanabe, Q. Cao, H. Tanaka, and Y. Ono, ''Double-filter high-resolution soft X-ray tomographic diagnostic for investigating electron acceleration in TS-6 reconnection merging experiments,'' *Rev. Sci. Instrum.*, vol. 92, no. 8, Aug. 2021, Art. no. 083504.

[10] J. Zhang, H. Qi, D. Jiang, M. He, Y. Ren, M. Su, and X. Cai, "Acoustic tomography of two dimensional velocity field by using meshless radial basis function and modified Tikhonov regularization method," *Measurement*, vol. 175, Apr. 2021, Art. no. 109107.
[11] X. Yun, J. He, A. Carevic, I. Slapnicar, J. Barlow, and M. Almekkawy, "Reconstruction of ultrasound tomography for cancer detection using total least squares and conjugate gradient method," *Proc. SPIE*, vol. 10580, pp. 125–135, Mar. 2018.
[12] A. Puri and S. Kumar, "An OMP-TV2 algorithm for detecting white matter fiber crossings in brain MRI," *Psychiatry Res., Neuroimag.*, vol. 321, Apr. 2022, Art. no. 111448.
[13] T. Hugger, B. Zahneisen, P. LeVan, K. J. Lee, H.-L. Lee, M. Zaitsev, and J. Hennig, "Fast undersampled functional magnetic resonance imaging using nonlinear regularized parallel image reconstruction," *PLoS ONE*, vol. 6, no. 12, Dec. 2011, Art. no. e28822.
[14] Y. Li, M. Gao, R. He, Y. Ren, H. Liu, L. Guo, and G. Xu, "Hemodynamic parameter estimation from magnetic resonance perfusion imaging with the Tikhonov regularization method," *IEEE Trans. Magn.*, vol. 51, pp. 1–4, 2015.
[15] Y. Liu and Y. Zhong, "Machine learning-based seafloor seismic prestack inversion," *IEEE Trans. Geosci. Remote Sens.*, vol. 59, pp. 4471–4480, 2021.
[16] H. Schwilden, J. Honerkamp, and C. Elster, "Pharmacokinetic model identification and parameter estimation as an ill-posed problem," *Eur. J. Clin. Pharmacol.*, vol. 45, pp. 545–550, Jan. 1993.
[17] T. Arikuma, S. Yoshikawa, R. Azuma, K. Watanabe, K. Matsumura, and A. Konagaya, "Drug interaction prediction using ontology-driven hypothetical assertion framework for pathway generation followed by numerical simulation," *BMC Bioinf.*, vol. 9, p. 1, Jan. 2008.
[18] A. Bjorck, *Numerical Methods for Least Squares Problems*. Philadelphia, PA, USA: SIAM, 1996.
[19] S. Boyd and L. Vandenberghe, *Convex Optimization*. New York, NY, USA: Cambridge Univ. Press, 2004.
[20] L. Shampine and M. Reichelt, "The MATLAB ode suite," *SIAM J. Sci. Comput.*, vol. 18, p. 1, Jan. 1997.
[21] Y. Aoki, "Study of singular capillary surfaces and development of the cluster newton method," Ph.D. thesis, UWSpace, 2012. [Online]. Available: http://hdl.handle.net/10012/6908
[22] M. C. Haaz, L. Rivory, C. Riche, L. Vernillet, and J. Robert, "Metabolism of irinotecan (CPT-11) by human hepatic microsomes: Participation of cytochrome P-450 3A and drug interactions," *Cancer Res.*, vol. 58, pp. 468–472, 1998.
[23] S. Willmann, K. Höhn, A. Edginton, M. Sevestre, J. Solodenko, W. Weiss, J. Lippert, and W. Schmitt, "Development of a physiology-based whole-body population model for assessing the influence of individual variability on the pharmacokinetics of drugs," *J. Pharmacokinetics Pharmacodyn.*, vol. 34, no. 3, pp. 401–431, Jun. 2007.
[24] A. Konagaya, *Bioinformatics*. Tokyo, Japan: The Institute of Electronics, Information, and Communication Engineering, 2009.

LUONG THI THEU was born in Thái Bình, Vietnam, in 1990. She received the B.Sc. degree in physics from Hanoi Pedagogical University 2 (HPU2), Hanoi, Vietnam, in 2012, and the M.Sc. and Ph.D. degrees in theoretical and mathematical physics from HPU2, in 2015 and 2021, respectively. She is currently employed as a Researcher with the Institute of Applied Technology, Thu Dau Mot University (TDMU). Her main research interests include physical models for biomedical systems and 2-D materials for gas sensors used for early cancer detection.

TRAN QUANG-HUY was born in Hanam, Vietnam, in 1985. He received the B.Sc. degree in physics from Hanoi Pedagogical University 2 (HPU2), Hanoi, Vietnam, in 2009, and the M.Sc. and Ph.D. degrees in electronics and telecommunication technology from the VNU University of Engineering and Technology (VNU UET), Hanoi, in 2013 and 2019, respectively. He is currently a Principal Lecturer with the Faculty of Physics, HPU2. His research interest includes biomedical signal processing such as ultrasound tomography (UT), magnetic resonance imaging (MRI), and electron paramagnetic resonance (EPR).

TRAN DUC-TAN (Member, IEEE) is currently an Associate Professor and the Vice Dean of the Faculty of Electrical and Electronic Engineering, Phenikaa University. He has published over 150 research articles. His main research interests include the representation, processing, analysis, and communication of information embedded in signals and datasets. He was a recipient of the award for the Excellent Young Researcher from Vietnam National University, Hanoi, in 2008, and the Third Prize in the contest "Vietnamese Talents," in 2008. His publications received the Best Paper Awards from the 9th International Conference on Multimedia and Ubiquitous Engineering (MUE-2015) and the International Conference on Green and Human Information Technology (ICGHIT-2015). He serves as the TP co-chair, technical committee program member, track chair, session chair, and reviewer of many international conferences and journals.

BHISHAM SHARMA is currently an Associate Professor with the Department of Computer Science and Engineering, Chitkara University, Punjab, India. He is a member of the Chitkara University Research and Innovation Network (CURIN). He is having 14 years of teaching and research experience at various reputed universities in India. His research interests include mobile computing, cloud computing, quantum computing, wireless communication, wireless sensor networks, wireless mesh networks, next-generation networking, network security, the Internet of Things, UAV, medical image processing, and edge/fog computing, in which he has published over 80 research papers in reputed SCI- and Scopus-indexed journals, international conferences, and book chapters.

SUBRATA CHOWDHURY (Member, IEEE) is with the Sreenivasa Institute of Technology and Management Studies, Chittoor, Andhra Pradesh, India. He has edited five books in association with the CRC Press and others. He has published more than 50 articles in international and reputed journals. His research interests include data mining, big data, machine learning, quantum computing, fuzzy logic, AI, edge computing, swarm intelligence, and healthcare. He was a member of the IET. He has received awards and nominations from different national and international science societies. He serves as a reviewer for IEEE TRANSACTIONS, Elsevier, and Springer, and an Academic Editor for Hindawi journals.

KARTHIK CHANDRAN (Senior Member, IEEE) was born in Madurai, Tamil Nadu, India, in 1986. He received the B.E. degree in electronics and instrumentation engineering from the Kamaraj College of Engineering and Technology, India, in 2007, and the master's and Ph.D. degrees in control and instrumentation engineering from the Kalasalingam Academy of Research and Education (KARE), in 2011 and 2017, respectively. In 2011, he joined the Department of Instrumentation and Control Engineering, KARE, India, as an Assistant Professor. He served as a Lecturer with the Department of Electrical and Computer Engineering, University of Woldia, Ethiopia, from 2016 to 2018. He is currently a Postdoctoral Researcher with Shanghai Jiaotong University, China. He is also an Associate Professor in mechatronics engineering with the Jyothi Engineering College, Kerala. He is current research interests include time delay control problems, nonlinear system identification, cascade control systems, and unmanned vehicles. He is a member of ACM.

SARAVANAKUMAR GURUSAMY (Senior Member, IEEE) was born in Seithur, Tamil Nadu, India. He received the B.Eng. degree in electronics and instrumentation engineering from the National Engineering College, Kovilpatti, India, in 2004, the master's degree in control and instrumentation engineering from the Thiagarajar College of Engineering, Madurai, in 2007, and the Ph.D. degree from the Faculty of Instrumentation and Control Engineering, Kalasalingam Academy of Research and Education (KARE), India, in 2017. In 2009, he joined the Department of Instrumentation and Control Engineering, KARE, as a Lecturer. In 2011, he became an assistant professor. From 2014 to 2018, he was a Lecturer with the Department of Electrical and Computer Engineering, University of Gondar, Ethiopia. Then, he rejoined KARE, as a Senior Assistant Professor, where he served for a year. He is currently an Associate Professor with the Department of Electrical and Electronics Technology, FDRE Technical and Vocational Training Institute (formerly Ethiopian Technical University), Addis Ababa, Ethiopia. His current research interests include biosensors, virtual instrumentation, applications of evolutionary algorithms for control problems, nonlinear system identification, multivariable PID controllers, model predictive control, autonomous vehicles, and mobile robotics.